A Magnetic Flux-Based Position Sensor for Control of an Electromechanical VVT Actuator

Ryan R. Chladny, *Student Member, IEEE* and Charles R. Koch, *Member, IEEE*

***Abstract*— A promising method for enhancing automotive internal combustion engine efficiency uses solenoid actuators to directly control gas exchange valves. Mitigation of valve seating velocities is challenging due to phenomena such as magnetic saturation and pressure disturbances. Production implementation of an electromagnetic valvetrain will require the development of cost effective yet accurate sensors for robust feedback control. A method of magnetic flux-based armature position measurement is presented. An overview of the modeling and control design is shown with experimental and simulated results using such a sensor configuration.**

I. INTRODUCTION

Traditional internal combustion engine (ICE) gas exchange valve timing is mechanically fixed with respect to crankshaft position. This timing determines when the valves open and close, thereby affecting the air-fuel mixture and exhaust flow. Since timing cannot be easily altered without significant engine modifications, a compromise between low and high engine speed efficiency is usually assigned [1]. A promising method of improving efficiency is through independent control of gas exchange valve timing. Although variable valve timing (VVT) has been recognized as a potential method to improve ICE performance as early as 1899 [2], relatively low fuel costs and emissions standards have not warranted the added engine complexity and cost. Recently however, a confluence of increasing fuel prices, stringent emissions standards, efficient power-electronics and affordable microprocessor and sensor technologies have motivated researchers to investigate the viability of variable valve timing methods. These include electrical motor [3], [4], pneumatic [5], [6], hydraulic [7], [8], and solenoid valve actuators [9], [10].

Solenoid actuators offer advantages over other actuator types with respect to precise regulation of transient cylinder charge and energy efficiency. Such actuators are generally comprised of a linear-moving armature between two flat pole face E-core magnets and two preloaded springs as described in [11].

Other solenoid designs include hinged or clapper-type configurations [13], [14], such as the prototype used in this work. An example of a typical hinged solenoid actuator is shown in Figure 1. The armature is mechanically linked between a torsion bar and linear compression spring. These springs are used to provide rapid flight times, overcome

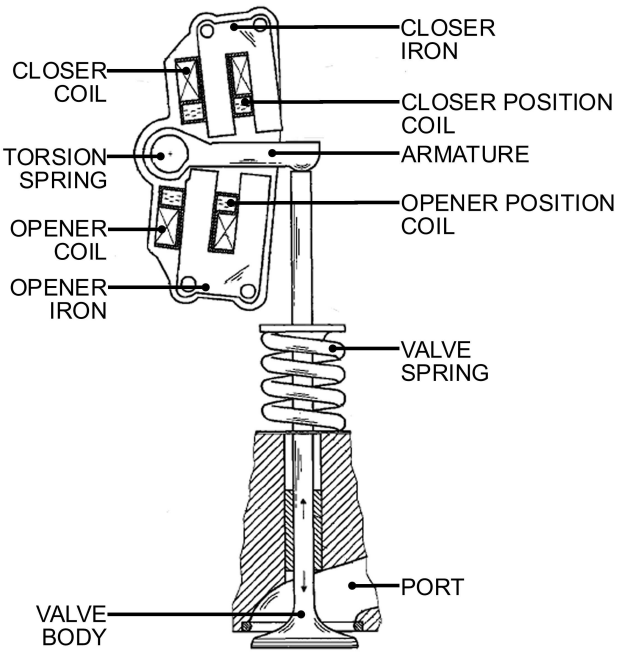

Fig. 1. Hinged Electromagnetic Gas Exchange Valve Actuator [12]

significant combustion pressures and minimize the necessary electrical energy input. Pole geometry is considered 'U' shaped and both the armature and core are fabricated from laminated steel for eddy current suppression. One of the primary remaining challenges of production implementation of an electromagnetic valvetrain (EMV) is the achievement of soft valve landing, particularly while subject to practical engine constraints. Armature and valve seating velocities of 0.1m/s are required to prevent premature engine wear and excessive acoustic emissions. It is also critical to minimize the valve transition time. Ideally this time should not exceed 5ms in order to accommodate a sufficiently high engine speed. It is also expected that a maximum excitation potential of 42V, the new on-board standard, will be available. To satisfy these performance and operating constraints, closed-loop control is required [15], [16], [17]. Closed-loop control is also necessary to compensate for system uncertainties including large disturbance forces from combustion pressure and parameter variation due to temperature change and component wear. Upon identification of system dynamics and control performance objectives, bandwidth and resolution requirements of a feedback sensor and/or output estimation method may be specified. In this article, an overview of

This work was supported in part by the Natural Sciences and Engineering Research Council of Canada, under Research Grant number 249553-02.

The authors would like to thank DaimlerChrysler for the donation of the solenoid valves.

R.R. Chladny and C.R. Koch are with the Department of Mechanical Engineering, University of Alberta (e-mail: rchladny@ualberta.ca; bob.koch@ualberta.ca).

proposed feedback techniques are presented along with preliminary simulation and experimental results of an alternative cost-effective method of flux-based position measurement. Unlike other applications where flux is a control state, such as induction motor control, here position and velocity are required for control constraints and trajectory tracking.

II. Feedback Constraints and Possible Sensor Candidates

Due to the low-impact speed requirement of the valve and significant combustion pressure fluctuations, a means of accurately sensing armature or valve position is required for feedback control. In [15] it was demonstrated that a sensor accuracy of at least $10\mu m$ is required. Presently, a sensor with this accuracy over a 8mm stroke length is either too expensive, unsuitable for under-hood environments or otherwise unfeasible for on-board control. In addition, the sensor response speed must not limit the control system and consequently stability. Therefore, the sensor must have at least an equivalent response or bandwidth of the actuator system. Methods of state reconstruction through external valve and/or armature-based position measurements have been documented. These include position or velocity measurements via linear variable differential transducer (LVDT) [18], laser [19], [20], [21] or eddy current displacement sensors [22], [23].

Although these sensors provide sufficient precision, accuracy and response, efforts are being made to develop alternative cost effective sensors or sensing methods with equivalent performance. These include the flux-based coil type [24], [14], [25], [26], [27], [28], observer based [29], [30] and self inductive [31], [32]. In the latter cases, it is proposed that the driving coil itself be used to relate the measured rate of change of induced coil current to the armature position and velocity. This may be done by momentarily deactivating the drive coil and relating velocity-induced currents to position. However, this method is susceptible to noise and signal processing challenges in addition to temporary loss of control authority [31] and thus potentially compromising tracking performance.

Observer based state reconstruction makes use of the measured current signal and estimated initial state conditions to predict plant output. Such schemes are sensitive to initial state estimates and require high gain for the relatively rapid estimation convergence required, making them prone to instability when subjected to excessive noise or disturbances. Thus, they are perhaps better suited to compensate for relatively slow parameter variations with adaptive feed-forward control.

Another feedback system demonstrated uses a microphone to adaptively improve impact speeds from sound intensity measurement [33]. Although proven successful in laboratory testbench experiments, such a sensor scheme is likely not practical in an engine environment due to associated sensor cost, multiple valves in operation and other acoustic sources.

III. Flux Sensor

Flux-based coil type sensors such as proposed in [25], appear to be a promising method of achieving a low-cost yet high-performance position measurement. The system incorporates a secondary sensor coil concentric to each of the opener and closer magnet drive coils. These sensor coils are terminated across high impedance analog integration and amplifier circuits. The circuit output signal can thus be related to magnetic flux. Using this signal with the drive current signal, position may be predicted through an inductance model. In the case of devices with variable air gaps such as solenoid actuators, the inductance is highly dependant on armature and hence valve position. Thus, any time-varying magnetic field produced by the excitation coil will induce an electromotive force (EMF) in the secondary coil as predicted by Faraday's law of mutual inductance. To account for analog drift, each channel is calibrated prior to excitation and the integration hardware is reset externally when the armature is at the opposite pole face of the coil in use. The reset of the integrator is particularly effective due to the periodic motion of the valve.

A. Nonlinear Inductance Model

As a means of providing an accurate model of the physical system, magnetic material saturation is considered. Saturation effects will be present at high magnetomotive force (MMF) values, particularly at small armature/pole face air gaps and/or high current excitation [34]. Control is expected to be executed while the system is at such operating conditions.

The following function is intended to approximate the flux linkage response with magnetic material saturation [35]:

$$\lambda(x,i) = \psi(1 - e^{-ig(x)}) \tag{1}$$

where i and $x\epsilon[-4\ 4]$mm represent coil current and armature position respectively and

$$g(x) = \frac{\beta}{\kappa - x} + \alpha. \tag{2}$$

A valve position of $x = 0$ corresponds to a mid-stroke valve and armature position. Using this form, the parameters ψ, β, κ and α are solved using a nonlinear least squares fit to FEA simulated data [34].

Assuming the sensor coil is measured with high impedance circuitry, resistance of the flux loop is negligible and the induced voltage due to a change in excitation current or flux may be expressed as:

$$v_{sc} = N_{sc}\frac{d\phi(i,x)}{dt} = \frac{N_{sc}}{N_{ec}}\frac{d\lambda(i,x)}{dt}, \tag{3}$$

where v_{sc} is the induced voltage in the sensor coil, $\frac{d\phi}{dt}$ is the flux induced potential and N_{sc} and N_{ec} are the respective number of turns for the sensor coil and excitation coil. In practice, the induced voltage is integrated (analog) and sampled. Thus, the integrated result may be expressed as:

$$\lambda = N_{ec}(\phi_o + \frac{\int v_{sc}dt}{N_{sc}}), \tag{4}$$

where ϕ_o is the initial flux condition prior to integration. Using the derived flux model, a relationship between current, flux and armature position is of the form:

$$x = \frac{\beta i}{\alpha i + ln(1 - N_{ec}(\phi_o + \int v_{sc} dt / N_{sc})/\psi)} + \kappa \quad (5)$$

Although the induction model appears sufficient for analytic control design, improved position accuracy has been observed through the direct use of FEA generated position, flux and excitation data in a look-up table algorithm. Note that a position measurement can only be observed with a non-zero current being applied. Current must be non-zero in order to satisfy controllability conditions [35].

B. State Space Model

1) Electrical Subsystem: The hinged actuator electrical domain may be represented by an RL circuit described by Faraday's law of induction and the following KVL equation:

$$\begin{aligned} v =& iR + \frac{d\lambda(i,x)}{dt} \\ =& iR + \psi e^{-i(\frac{\beta}{\kappa - x} + \alpha)} \left((\frac{\beta}{\kappa - x} + \alpha) \frac{di}{dt} \right. \\ & \left. + \frac{\beta i}{(\kappa - x)^2} \frac{dx}{dt} \right), \end{aligned} \quad (6)$$

with applied voltage, v, and excitation coil winding resistance, R.

Solving for rate of change of current yields:

$$\frac{di}{dt} = \frac{-\beta \psi i \dot{x} + e^{i(\frac{\beta}{\kappa - x} + \alpha)} (\kappa - x)^2 u}{\psi(\beta + \alpha(\kappa - x))(\kappa - x)} \quad (7)$$

where the input, u, is defined as $u = v - iR$.

2) Mechanical Subsystem: The nonlinear inductance model in (1) is used to develop a relationship between magnetic force, air gap and current through co-energy [36]. To derive the co-energy of the system, W_c, flux is integrated with respect to current i:

$$\begin{aligned} W_c(x,i) =& \frac{\psi e^{-i(\frac{\beta}{\kappa - x} + \alpha)}}{\beta + \alpha(\kappa - x)} \left(\kappa + e^{i(\frac{\beta}{\kappa - x} + \alpha)} (\beta i \right. \\ & \left. + (-1 + \alpha i)(\kappa - x)) - x) \right) \end{aligned} \quad (8)$$

Differentiating W_c with respect to x yields the expression for magnetic force:

$$\begin{aligned} F_m(x,i) =& \frac{\partial W_c(x,i)}{\partial x} \\ =& \frac{\psi e^{-i(\frac{\beta}{\kappa - x} + \alpha)}}{(\beta + \alpha(\kappa - x))^2 (\kappa - x)} (-\beta i + (-1 \\ & + e^{i(\frac{\beta}{\kappa - x} + \alpha)} - \alpha i)(\kappa - x) \Big) \end{aligned} \quad (9)$$

Applying Newton's second law, valve motion as a function of magnetic force, torsion bar force and viscous damping is derived:

$$\begin{aligned} \ddot{x}(m_v + \frac{I_o}{\ell_v^2}) + \dot{x}(b_v + \frac{\hat{b}}{\ell_v^2}) + x(k_v + \frac{\hat{k}}{\ell_v^2}) \\ + F_v + F_g = \frac{F_m(i,x) \ell_m}{\ell_v}, \end{aligned} \quad (10)$$

where:

- m_v is the effective valve and moving spring mass
- ℓ_v is the radial distance from the armature pivot point to where the longitudinal armature and valve axes intersect
- I_o is the armature and torsion bar moment of inertia about the pivot point
- b_v is the viscous damping coefficient associated with the valve
- $\hat{b}$ is the viscous damping coefficient associated with the armature
- k is the valve spring constant
- $\hat{k}$ is the angular torsion bar spring constant
- F_v is the valve spring pre-load
- F_g is the time and position dependant gas force acting upon the valve
- F_m is the magnetic force on the armature
- ℓ_m is the radial distance from the armature pivot point to where the resultant magnetic force acts on the armature

Letting $\bar{x} = \kappa - x$ and substituting the expression for magnetic force, (9), into (10) results in:

$$\begin{aligned} & \ddot{x}m + \dot{x}b + xk + F_v + F_g \\ & = \frac{\ell_m \psi e^{-i(\frac{\beta}{\bar{x}} + \alpha)}}{\ell_v (\beta + \alpha \bar{x})^2 \bar{x}} \left(-\beta i + (-1 + e^{i(\frac{\beta}{\bar{x}} + \alpha)} - \alpha i) \bar{x} \right), \end{aligned} \quad (11)$$

with $m = m_v + \frac{I_o}{\ell_v^2}$ representing the effective system mass, $k = k_v + \frac{\hat{k}}{\ell_v^2}$ the effective spring constant and $b = b_v + \frac{\hat{b}}{\ell_v^2}$ the effective damping coefficient.

Note that the magnetic force, F_m, considers only a single magnet in isolation. This assumption is considered reasonable due to the high permeability of the armature and, since in practice, only one coil is active at any time. Sufficiently small angles are assumed such that $\sin\theta \sim \theta$ since θ is limited to less than $|\pm 7^o|$. Note that external forces such as those caused by gravity, engine and vehicle dynamics are considered negligible.

Finally, defining the state vector $\mathbf{x} = [i \ \bar{x} \ \dot{x}]^T$ results in the following nonlinear state space model

$$\begin{aligned} f(x) = & \begin{bmatrix} \frac{-\beta x_3}{(\beta + \alpha x_2) x_2} & 0 & 0 \\ 0 & 0 & 1 \\ \frac{-\ell_m \beta \psi e^{-x_1(\frac{\beta}{x_2} + \alpha)}}{\ell_v m (\beta + \alpha x_2)^2 x_2} & \frac{k}{m} & -\frac{b}{m} \end{bmatrix} \mathbf{x} \\ & + \begin{bmatrix} 0 \\ 0 \\ \frac{-\kappa k}{m} - \frac{(F_v + F_g)}{m} \\ + \frac{\ell_m \psi e^{-x_1(\frac{\beta}{x_2} + \alpha)}}{\ell_v m (\beta + \alpha x_2)^2} \left(-1 + e^{x_1(\frac{\beta}{x_2} + \alpha)} - \alpha x_1 \right) \end{bmatrix}, \end{aligned} \quad (12)$$

$$g(x) = \begin{bmatrix} \frac{e^{x_1(\frac{\beta}{x_2} + \alpha)} x_2}{\psi(\beta + \alpha x_2)} \\ 0 \\ 0 \end{bmatrix} u, \quad (13)$$

and the output equation:

$$h(x) = [0 \ 1 \ 0] \begin{bmatrix} x_1 \\ x_2 \\ x_3 \end{bmatrix}. \quad (14)$$

Note that this system is in control affine form

$$\begin{aligned}\dot{\mathbf{x}} &= f(x) + g(x)u \\ y &= h(x)\end{aligned} \tag{15}$$

IV. Flat Output Linearization

It can be shown that the nonlinear induction plant model is differentially flat. A system may be considered (differentially) flat if the state(s) and input(s) may be expressed explicitly as a function of the output(s) and a finite number of output time derivatives. This endogenous feedback results in an equivalent linearization and thus linear tracking error dynamics are attainable for a closed loop system [37], [38]. As was done for a linear actuator in [23], [35], a voltage control scheme is derived for the hinged actuator (coil dynamics are invoked so that voltage is the control output).

A. Voltage Control

With reference to the nonlinear induction plant model defined by (12) and (13), armature position, x_2, may be taken as the plant flat output, y. As a method of incorporating coil dynamics in the flatness control scheme, voltage is sought as the differentially flat plant input. Taking consecutive time derivatives of the position output, y, yields the following relationships:

$$\begin{aligned}\dot{y} &= \dot{x}_2 = x_3 \\ \ddot{y} &= \dot{x}_3 = -\frac{b}{m}x_3 + \frac{k}{m}(x_2 - \kappa) - \frac{(F_v + F_g)}{m} \\ &\quad + \frac{\psi e^{-x_1(\frac{\beta}{x_2}+\alpha)}}{(\beta+\alpha x_2)^2 x_2}\Big(-\beta x_1 + (-1 + e^{x_1(\frac{\beta}{x_2}+\alpha)} \\ &\quad -\alpha x_1)x_2\Big) \\ y^{(3)} &= \dddot{x}_3 = -\frac{b}{m}\ddot{y} + \frac{k}{m}\dot{y} - \frac{\dot{F}_g}{m} + \frac{\dot{F}_{mag}}{m}\end{aligned} \tag{16}$$

where

$$\begin{aligned}\dot{F}_{mag} = &-\frac{1}{\ell_v y^3(\beta+\alpha y)^3}(\beta e^{-x_1(\frac{\beta}{y}+\alpha)}\ell_m\psi(\\ &- x_1 y(\beta+\alpha y)^3\dot{x}_1 + (\beta^3 x_1^2 + 2\alpha\beta^2 x_1(-2\alpha x_1)y^2 \\ &+ 2\alpha(-1 + e^{x_1(\frac{\beta}{y}+\alpha)} - \alpha x_1)y^3)\dot{y})).\end{aligned} \tag{17}$$

Finally, voltage may be determined as a function of armature position (and subsequent time derivatives) and current by replacing $\dot{x}_1$ with the expression for coil dynamics given in 7. Note that a singularity occurs for zero current, $i = x_1 = 0$). If $y^{(3)}$ is chosen as:

$$y^{(3)} = -k_1(y - y_r) - k_2(\dot{y} - \dot{y}_r) - k_3(\ddot{y} - \ddot{y}_r) + y_r^{(3)},$$

where y_r represents a reference trajectory. Defining tracking error as, $e = y - y_r$, the following exponentially stable tracking closed loop error dynamics are rendered:

$$e^{(3)} + k_3\ddot{e} + k_2\dot{e} + k_1 e = 0 \tag{18}$$

In practice, the inductance of the magnetic response is sufficiently high so that voltage may be regulated through interpreting the controller output as a high frequency PWM duty cycle (42V corresponds to 100% duty cycle).

B. Reference Trajectory Design

Upon control law derivation, optimal reference trajectories are sought subject to physical and practical constraints. The MATLAB optimization routine `fmincon.m` is used to optimize B-spline coefficients used to parameterize a fifth order trajectory set subject to physical constraints. A model based cost function is used to minimize electromagnetic force. A detailed description of the method is provided in [35] for a linear actuator.

V. Evaluation of Flux Sensor Performance

Prior to experimental testing, the flux-based position sensor was evaluated in simulation using both the derived analytic function and FEA data in look-up table form.

A. Modeling

A MATLAB Simulink model capable of directly using experimental and ANSYS simulated data to predict the hinged actuator behavior has been designed. A similar model has been validated experimentally (including an eddy current model) for a linear-motion VVT actuator while undergoing an opening cycle as shown in [34]. The model is particularly useful for predicting controller performance while using the flux position sensor and velocity estimation. The model may be considered a hybrid FEA-analyitc lumped parameter model as, technically, it is neither but incorporates elements of both in an attempt to use the accuracy of a field solution with the relative computational simplicity of solving a system of ODEs. Thus, it has greater accuracy than a strictly ODE based model, but is not amenable to analytic control design. Rather, its primary purpose is to simulate the experimental conditions for evaluating control performance with model-experiment mismatch.

B. Simulated Controller Performance

Using the derived flat output voltage controller and reference trajectories, initial simulations were conducted contrasting full state feedback (FSFB) performance with state estimation via flux-based FEA look-up tables and Kalman filtering (position and velocity respectively). Position and velocity estimates are sampled with a zero order hold to approximate digital sampling. Figures 2 and 3 indicate mechanical and electrical response respectively. When position and velocity reconstruction was used, the landing performance was degraded with respect to impact speed, landing time and energy input. However, the results obtained still satisfied the respective performance constraints. In addition, analytic and FEA-based sensor performance is contrasted with FSFB results in Figure 4. It was observed that for regions closer to the pole face, the analytic and FEA-based estimates were nearly identical. In fact, analytic model accuracy could be improved by fitting to selective operating regions. In the case shown, the fit was performed over a region not exceeding 4mm away from the pole face and at current levels of less than 15A (where landing control is generally implemented). Simulated analytic error was in excess of 0.20mm for air gaps greater than 3mm. In contrast, the FEA based results

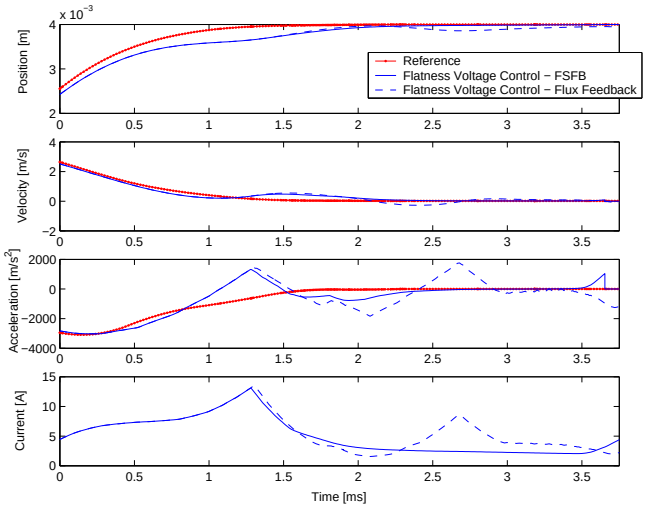

Fig. 2. Nominal landing controller dynamic results with FSFB and flux based position feedback

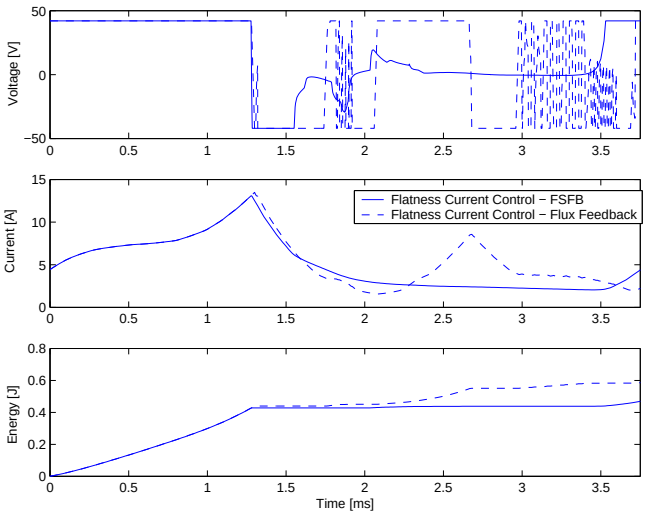

Fig. 3. Nominal landing controller input results with FSFB and flux based position feedback

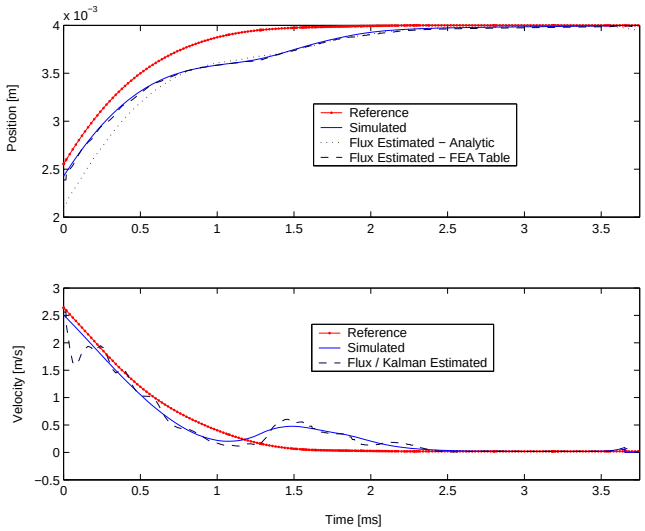

Fig. 4. Reference, simulated, analytic and FEA flux based position

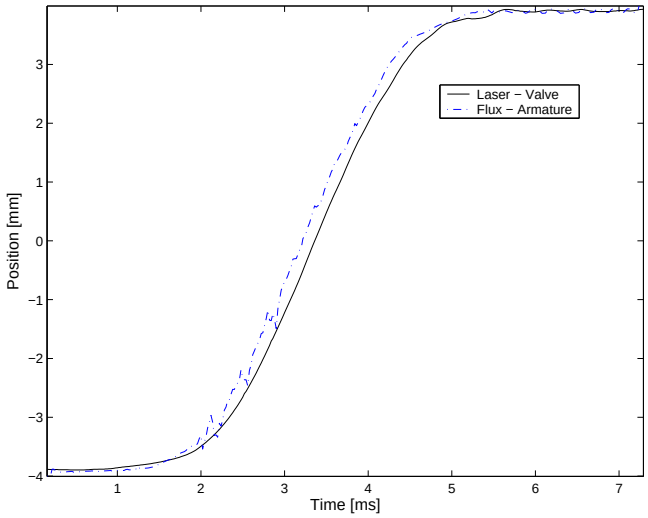

Fig. 5. Experimental FEA flux-based position estimation (closing)

exhibited a maximum error of approximately 0.08mm over a range of 6mm (region where current is non-zero) and was at least partially attributed to zero order hold sampling.

VI. Experimental Flux Sensor Performance

A preliminary experiment was established in which the flux-based position reconstruction algorithm was tested with basic PI landing and open-loop feedforward control. The actuator and valve are mounted to an actual single cylinder engine head for realistic tests. Armature position was compared to the valve position which was measured with a optoelectronic laser displacement sensor (resolution of $6\mu m$ and integration time of $200\mu s$). Without calibration, the FEA results, measured flux and current signals were used in the landing control algorithm as shown in Figure 5. Assuming no dynamics between the armature and valve, the average absolute error over a 4mm range was 0.04mm with a maximum of 0.4mm at a distance of 5mm from the pole face (and feedforward currents less than 5A). However, it should be noted that the difference in laser position and reconstructed position may in part be caused by the flexible lash adjuster and/or the laser response (set slower for a clean signal). In addition, it is suspected that this performance can be further improved through online calibration.

VII. Conclusions

A brief discussion of displacement sensors has been presented in contrast with a flux-based position measurement scheme. This displacement sensor offers a practical and economical method of predicting armature and valve position for closed loop landing control. By conducting numerical simulations, the method accuracy may be improved over analytic function approximations as shown through simulation.

In addition, preliminary experimental findings suggest that with further refinement, the sensing technique is feasible for flatness-based landing control with respect to the control objectives.

REFERENCES

[1] M. Schechter and M. Levin, "Camless engine," *SAE paper 960581*, 1996.

[2] D. Payne, "Electically controlled valve gear for gas or other motors," *U.S. Patent 623,821*, 1899.

[3] T. A. Parlikar, W. S. Chang, Y. H. Qiu, M. D. Seeman, D. J. Perreault, J. G. Kassakian, and T. A. Keim, "Design and experimental implementation of an electromagnetic engine valve drive," *IEEE / ASME Trans. Mechatronics*, vol. 10, pp. 482–494, 2005.

[4] R. Henry, "Single-cylinder engine tests of a motor-driven variable-valve actuator," *SAE paper 2001-01-0241*, 2001.

[5] W. Richeson and F. Erickson, "Pneumatic actuator with permanent magnet control valve latching," *U.S. Patent No. 4,852,528*, 1989.

[6] L. Gould, W. Richeson, and F. Erickson, "Performance evaluation of a camless engine using valve actuators with programmable timing," *SAE paper 910450*, 1991.

[7] J. Allen and D. Law, "Production electro-hydraulic variable valve-train for a new generation of I.C. engines," *SAE paper 2002-01-1109*, 2002.

[8] S. Barros da Cunha, J. Hedrick, and A. Pisano, "Variable valve timing by means of a hydraulic actuation," *SAE paper 2000-01-1220*, 2000.

[9] M. Pischinger, W. Salber, F. van der Staay, H. Baumgarten, and H. Kemper, "Benefits of the electromechanical valve train in vehicle operation," *SAE paper 2000-01-1223*, 2000.

[10] B. Lequesne, "Fast acting, long-stroke solenoids with two springs," *IEEE Trans. Ind. Applicat.*, vol. 26, pp. 848–856, 1990.

[11] P. Gladel, F. Kreitmann, O. Meister, T. Stolk, and A. V. Gaisberg, "Aktor zur elektromagnetischen Ventilsteuerung," *German Patent Application DE19961608 A1*, 1999.

[12] T. Stolk and A. Gaisberg, "Elektromagnetischer aktuator," *German Patent Application DE 10025491 A1*, 2001.

[13] Y. Kawase, H. Kikuchi, and S. Ito, "3-D nonlinear transient analysis of dynamic behavior of the clapper type DC magnet," *IEEE Trans. Magn.*, vol. 27, no. 5, pp. 4238–4241, 1991.

[14] M. Montanari, F. Ronchi, C. Rossi, and A. Tonielli, "Control of a camless engine electromechanical actuator: Position reconstruction and dynamic performance analysis," *IEEE Trans. Ind. Electron.*, vol. 51, pp. 299–311, 2004.

[15] C. Koch, A. Lynch, and R. Chladny, "Modeling and control of solenoid valves for internal combustion engines," *2nd IFAC Conf. on Mechatronic Systems*, pp. 317–322, 2002.

[16] Y. Wang, "Camless engine valvetrain: Enabling technology and control techniques," *Ph.D. thesis, University of California at Santa Barbara*, 2001.

[17] J. Savage and J. Matterazzo, "Application of design of experiments to determine the leading contributors to engine valvetrain noise," *SAE paper 930884*, 1993.

[18] Z. Sun and D. Cleary, "Dynamics and control of an electro-hydraulic fully flexible valve actuation system," *Proceedings of the American Control Conference*, vol. 4, pp. 3119–3124, 2003.

[19] C. Tai and T. Tsao, "Control of an elctromechanical actuator for camless engines," *Proc. 2003 American Control Conference*, 2003.

[20] Y. Wang, T. Megil, M. Haghgooie, K. Peterson, and A. Stefanopoulou, "Modeling and control of electromechanical valve actuator," *SAE paper 2002-01-1106*, 2002.

[21] A. Stubbs, "Modeling and controller design of an electromagnetic engine valve," *Master's thesis, University of Illinois at Urbana-Champaign*, 2000.

[22] K. Peterson, J. Grizzle, and A. Stefanopoulou, "Nonlinear control for magnetic levitation of automotive engine vale (sic)," *IEEE Trans. Contr. Syst. Technol.*, vol. 14, pp. 346–354, 2006.

[23] S. Chung, "Flatness-based voltage end control of a gas exchange solenoid actuator for IC engines," *M.Sc. thesis, Dept. Mechanical Engineering, University of Alberta*, 2005.

[24] A. Scacchioli, "Hybrid regulation of electromagnetic valves in automotive systems," *Ph.D. thesis, Dept. of Electrical Engineering, University of LAquila*, 2005.

[25] F. Ronchi and C. Rossi, "Sensing device for camless engine electromagnetic actuators," *Proceedings of the IEEE International Conference on Industrial Electronics Control and Instrumentation (IECON)*, pp. 1669–1674, 2002.

[26] C. Rossi and T. Alberto, "Method and device for estimating the position of an actuator body in an electromagnetic actuator to control a valve of an engine," *Magneti Marelli European Patent Application EP 1152129 A1*, 2001.

[27] C. Rossi and A. Tonielli, "Method and device for estimating the position of an actuator body in an electromagnetic actuator to control a valve of an engine," *European Patent Application EP 1152129 A1*, 2001.

[28] T. Roschke and M. Bielau, "Verfahren zur modellbasierten Messung und Regelung von Bewegungen an elektromagnetischen Aktoren," *Technische Universitaet Dresden German Patent Application DE 19544207 A1*, 1995.

[29] A. Lynch, C. Koch, and R. Chladny, "Nonlinear observer design for sensorless electromagnetic actuators," *3rd International Conference on Dynamics of Continuous, Discrete and Impulsive Systems, May 2003*, 2003.

[30] P. Eyabi, "Modeling and sensorless control of solenoid actuators," *Ph.D. thesis, Dept. Mechanical Engineering, Ohio State University*, 2003.

[31] S. Butzmann, J. Melbert, and A. Koch, "Sensorless control of electromagnetic actuators for variable valve train," *SAE paper 2000-01-1225*, 2000.

[32] D. Takashi and M. Iwao, "Valve drive device for internal combustion engine and initial position setting method for valve element," *Japan Patent Application JP 0224624*, 1995.

[33] K. Peterson and A. Stefanopoulou, "Extremum seeking control for soft landing of an electromechanical valve actuator," *Automatica*, 2004.

[34] R. Chladny, C. Koch, and A. Lynch, "Modeling automotive gas-exchange solenoid valve actuators," *IEEE Trans. Magn.*, vol. 41, pp. 1155–1162, 2005.

[35] C. Koch, A. Lynch, and S. Chung, "Flatness-based automotive solenoid valve control," *6th IFAC Symp. Nonlin. Contr. Systems (NOLCOS)*, pp. 1091–1096, 2004.

[36] H. Woodson and J. Melcher, *Electromechanical Dynamics Part I: Discrete Systems*. John Wiley & Sons, 1968.

[37] J. Lévine, "On flatness necessary and sufficient conditions," *6th IFAC Symp. Nonlin. Contr. Systems (NOLCOS)*, pp. 125–130, 2004.

[38] P. Martin, R. Murray, and P. Rouchon, "Flat systems," *Mini-course given at the European Control Conference (ECC)*, 1997.